

## Charge of a macroscopic particle in a plasma sheath

A. A. Samarian and S. V. Vladimirov

*School of Physics, The University of Sydney, New South Wales 2006, Australia*

(Received 19 December 2002; published 20 June 2003)

Charging of a macroscopic body levitating in a rf plasma sheath is studied experimentally and theoretically. The nonlinear charge vs size dependence is obtained. The observed nonlinearity is explained on the basis of an approach taking into account different plasma conditions for the levitation positions of different particles. The importance of suprathermal electrons' contribution to the charging process is demonstrated.

DOI: 10.1103/PhysRevE.67.066404

PACS number(s): 52.27.Lw, 52.25.Gj, 52.27.Gr, 52.35.-g

### I. INTRODUCTION

Complex plasmas, i.e., plasmas containing macroscopic bodies (e.g., colloidal “dust” particles) in addition to electrons, ions, and neutrals, are open systems. Parameters of the macroscopic particle component such as particle charge thus appear as a function of not only their “internal” characteristics (size, shape, material, etc.), but also as a function of “external,” with respect to that component, plasma conditions (e.g., plasma density and temperature). The knowledge of the charge is in the foundation of the character of self-organized structures observed in a complex plasma such as Coulomb crystals, liquids, clusters, etc., as well as phase transitions between them [1–6]. These structures have recently attracted cross-disciplinary attention because of the similarities with processes in condensed matter physics, statistical physics, biophysics, etc. [7].

For typical plasma conditions, the charge can be reasonably predicted by the widely adopted “orbital-motion-limited” (OML) model, where the dust grain is considered as a spherical probe and the charging is due to plasma currents onto the grain surface [8,9]. The currents are calculated by assuming that the electrons and ions are collected when their mainly collisionless orbits intersect the probe surface. Usually, the electrons are assumed to be Boltzmann distributed, and the ions are shifted Maxwellian, taking into account their possible drift velocity in the external field [10]. The current balance determines the net particle charge which is negative and large, as related to the charges of plasma electrons and ions (such that the dimensionless charge  $Z_d = Q_d/e$  is of the order of  $10^3$ – $10^4$ ) [9]. In the simplest approximation of small ( $a \ll \lambda_{Di}$ , where  $\lambda_{Di}$  is the ion Debye length) spherical particles, their charge is  $Q_d = a\varphi_s$ , where  $\varphi_s$  is the surface potential [8,9]. If  $\varphi_s = \text{const}$ , we expect the particle charge to be directly proportional to its radius.

In most of the experiments, the dust particle structures levitate in the sheath region of a radio-frequency (rf) discharge plasma. Sophisticated experimental methods have been recently developed [11–16] to elucidate the charge on a dust grain. Most of the reported experimental data demonstrate nonlinear dependency of the particle charge on its size [14–16].

In this paper, we report on the experiments dedicated to clarify the dependence of the dust charge as a function of its size in a rf-discharge plasma. The experiments are complemented by modeling the charge behavior of a dust particle in

the sheath region. Among the possible contributions to the particle charging, we single out the effects of suprathermal electrons (STEs). We demonstrate that the presence of STEs can indeed cause the observed nonlinear behavior of the charge on the size of a levitating particle.

### II. EXPERIMENT

The experiments were carried out in a capacitively coupled rf discharge in argon. The experimental setup is shown in Fig. 1 and described in detail in Refs. [17,18]. The input power is 60–100 W and the resulting dc self-bias of the powered electrode is 5–25 V, measured at the electrical feedthrough. A compensated single Langmuir probe is used to make measurements of the plasma parameters. The typical plasma parameters in our experiments are the density  $n_e \sim (2-8) \times 10^8 \text{ cm}^{-3}$  and the temperature  $T_e \sim 1-1.5 \text{ eV}$ . The dust particles used in our experiments were spherical: melamine formaldehyde ( $\rho = 1.5 \text{ g/cm}^3$ , radius  $a = 1.45, 2.12, 2.83, 3.05, 3.52 \mu\text{m}$ ), carbon ( $\rho = 2.1 \text{ g/cm}^3$ ,  $a = 1.05 \mu\text{m}$ ), corundum ( $\text{Al}_2\text{O}_3$ ,  $\rho = 4.05 \text{ g/cm}^3$ ,  $a = 2.45 \mu\text{m}$ ), and glass balloons ( $\rho_{\text{eff}} = 0.8 \text{ g/cm}^3$ ,  $a = 5 \mu\text{m}$ ). The dust particles suspended in the plasma are illuminated using a helium-neon laser. The laser beam enters the discharge chamber through the side window mounted on the side port. The laser beam is expanded in the vertical directions into sheets of light by a system of cylindrical lens. This allows us to view the light scattered by the suspended

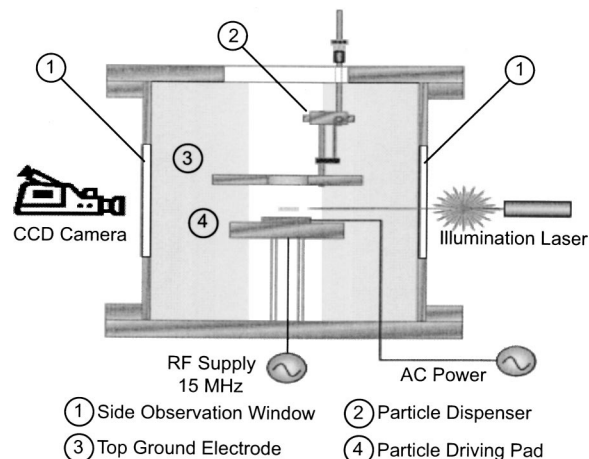


FIG. 1. The experimental setup.

dust particles. The particle positions are analyzed with a software program that outputs their vertical coordinates. The charges on the particles were measured by two techniques successfully used previously [18–20], namely, by the vertical equilibrium technique (VET) [18,19] and by the vertical resonance technique (VRT) [19,20].

The VET method operates with the equilibrium height of dust particles levitating in the sheath region. In the radial direction, the particles usually are trapped within the area of the ring electrode. The main forces acting on the dust particles levitating in the sheath region are the gravity force  $F_g$ , the electrostatic force  $F_{el}$ , the thermophoretic force  $F_{th}$ , and the ion drag force  $F_i$ . At the equilibrium position, the total force is equal to zero. The gravity force is  $F_g = m_d g \cong 5 \times 10^{-12}$  N. An estimate of the thermophoretic force gives  $F_{th} \leq 10^{-14}$  N, since the temperature gradient in the sheath does not exceed 5 K/cm. The upper limit of the ion drag force can be estimated to be  $F_i \approx 10^{-18}$  N [17]. Based on that, we can conclude that under the present conditions the gravity force is compensated almost entirely by the electrostatic force  $F_{el}$ . Thus the equilibrium condition can be written as  $m_d g = Q_d E$ , and the particle charge is given by  $Q_d = m_d g / E$ . The value of the electric field is then obtained using the parabolic sheath model; the general parabolic nature of the sheath for pressures more than 10 Pa has been clearly demonstrated in Refs. [14,19].

The VRT method uses the sinusoidal voltage (up to 500 mV) applied to the powered lower electrode. This leads to vertical oscillations of a dust particle. At low frequencies (a few hertz), the resonance in the vertical motion is observed. The value of the resonance frequency is used in conjunction with the parabolic sheath potential approximation to evaluate the charge  $W = \sqrt{Q_d E' / m_d}$ , where  $E'$  is the vertical gradient of the electric field. In the parabolic sheath approximation, the gradient was determined to be 1.2 V/m<sup>2</sup> in our experiment from the probe plasma potential measurement. The results of these methods are in good agreement [21], and therefore below in this paper we present only the values obtained by the VET.

Circles in Fig. 2 represent experimental dependence of the charge of the levitating melamine formaldehyde particle on its size for the 60 W of the input power and the pressure 18.3 Pa [Fig. 2(a)] and 12.1 Pa [Fig. 2(b)]. The obtained dependencies are strongly nonlinear: the obtained dependencies have the exponents 1.85, Fig. 2(a), and 1.66, Fig. 2(b). This result is in agreement with the data (the exponents are within the range from 1.7 to 2.5) reported earlier [14,16]. Such results highlight the problem of the charge vs size dependence.

### III. MODELING

In general, the particle charge can be written as  $Q_d = F(a) \varphi_s$ , where the function  $F(a)$  is not necessarily linear. On the other hand, the surface potential reflects plasma parameters taken by the particle as a kind of “probe” at the point of levitation. Indeed, from the current balance equation, the potential appears as  $\varphi_s = f^\varphi(n_e/n_i, T_e, v_i)$ . However, the plasma parameters are at the point of levitation and therefore the functions of the particle size, i.e.,  $n_e/n_i$

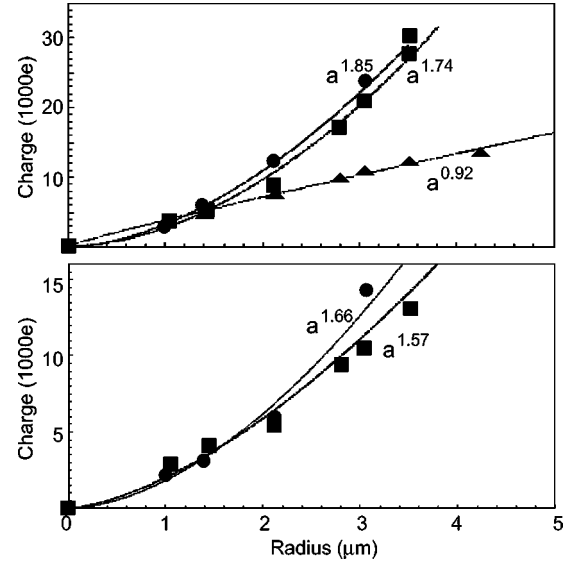


FIG. 2. Dependence of the charge of the levitating particle on its size. Circles represent experimental results, rectangles represent results of theoretical modeling with STEs, and triangles represent theoretical modeling without STEs.

$= f^n(h_{lev})$ ,  $T_e = f^T(h_{lev})$ , and  $v_i = f^v(h_{lev})$ , where in turn the levitation height  $h_{lev} = f^h(a)$ . Thus the surface potential is  $\varphi_s = f^\varphi(f^n(f^h(a)), f^T(f^h(a)), f^v(f^h(a)))$ . In an ideal experiment, when all particles are in the same plasma conditions (i.e.,  $\varphi_s = \text{const}$ ), the charge measurements can, in principle, give us the functional dependence  $F(a)$ . In reality, a measurement of a levitating charge  $Q_d$  as a function of the size  $a$  gives us the mixed dependence

$$Q_d \propto F(a) f^\varphi(f^n(f^h(a)), f^T(f^h(a)), f^v(f^h(a))). \quad (1)$$

From this consideration, we see that the particle charge indeed appears as a complex function of its size via the size dependence of the levitation height and the height dependence of the plasma parameters.

To elucidate the contribution of different functions ( $f_n^\varphi$ ,  $f_T^\varphi$ , and  $f_v^\varphi$ ) into the charge dependence on the radius of a levitating particle, we calculate the charge on the basis of the self-consistent hydrodynamic model of the dust levitation and equilibrium in the collisional plasma sheath taking into account plasma ionization. For more details of the model, see [22].

We consider one-dimensional configuration and choose plasma parameters taken from the experiment. All variables of interest are calculated self-consistently in the sheath as functions of the distance  $z$  from the electrode and given plasma parameters in the bulk, namely, the sheath potential  $\varphi(z)$ , the electric field  $\mathbf{E}(z) = \hat{\mathbf{z}}E(z) = -d\varphi(z)/dz$ , the ion flow velocity  $\mathbf{v}_i(z) = \hat{\mathbf{z}}v_i(z)$  and density  $n_i(z)$ , and the main electron density  $n_e(z)$  which is supposed to be Boltzmann distributed. We assume that the main electron temperature is constant in the whole region of interest. We also add the fraction of STEs, with the ratio of the STE density to the ion density at the electrode as a boundary condition. The boundary condition is determined by the secondary emission yield

taken as  $n_{eh}(0)/n_i(0)=0.045$  [23,24]. The model space distribution is taken in the form close to the step function in space, namely,  $n_{eh}=(n_0/2)\{\tanh[(z-z_0)/z_1]+1\}$ , where the shift of the step is  $z_0\sim z_{sh}$ , where  $z_{sh}$  is the sheath and presheath width, and the width of the step  $z_1\sim\lambda_{De}$ , where  $\lambda_{De}$  is the electron Debye length.

The sheath potential is determined by Poisson's equation; in this model, we neglect the total charge contributed by the dust grains (i.e., we assume the dust number density to be small). The ion dynamics is governed by the continuity and momentum equations. The continuity equation for the ions takes into account plasma production; the main mechanism of ionization is assumed to be electron impact ionization with the additional contribution of STE so that the effective plasma ionization source is proportional to the neutral gas, and contains "standard" contribution of plasma Boltzmann electrons with exponential of the inverse of the electron temperature [22,25], and additional STEs, contribution depending on the STE density and the STE temperature.

The momentum equation for the plasma ions takes into account the momentum transfer between ions and neutrals, and the main mechanism for the ion-neutral collisions is considered to be charge exchange. For low ion speeds, the momentum transfer rate is proportional to the ion speed, while for high ion speeds this rate is proportional to the square of the ion speed. The latter case applies in the sheath region in the calculations reported here, but not necessarily in the plasma bulk region. Assuming that the electrode has a constant potential, the model equations are numerically integrated to give the dependence of the potential, and thence of the sheath electric field, on the distance from the electrode  $z$ . The charge  $Q_d$  of the dust particles (which is dependent on the plasma parameters, in particular, on the local electric sheath potential, the velocity of the ion flow, and STEs) is found from the OML condition of zero total plasma current onto the grain surface. Applicability of the OML approximation in the case of anisotropic plasma is discussed in Refs. [19,26]. In general, it was noted in Ref. [27] that the experimental and theoretical trends are to prove that, for the applicability of the OML approach, one should have  $a\ll\lambda_{sc}$ , where  $\lambda_{sc}$  is the effective screening length. For our experimental conditions, this inequality is always maintained.

Here, we follow the approach of Ref. [10] and write the ion current onto the dust grain, taking into account the shifted Maxwell distribution of plasma ions, as

$$I_i=\pi a^2 e n_i(z) \bar{v}_i(z) \left[ 1 - \frac{2eQ_d(z)}{am_i \bar{v}_i^2(z)} \right], \quad (2)$$

where  $\bar{v}_i(z)=\sqrt{v_i^2(z)+8v_{Ti}^2/\pi}$ ,  $v_{Ti}^2=T_i/m_i$ , and  $T_i$  is in energy units (such that the Boltzmann constant is unity). Note that Eq. (2) takes place when  $v_i\gg v_{Ti}$ . Note that in the opposite limit, we have the OML result for the ion current,

$$I_i=\sqrt{8\pi} a^2 e n_0 v_{Ti} \left[ 1 - \frac{eQ_d(z)}{am_i v_{Ti}^2(z)} \right]. \quad (3)$$

The electron currents, taking into account the contribution of STEs, are given by

$$I_e(Q_d)=-\sqrt{8\pi} e a^2 n_0 \sqrt{\frac{T_e}{m_e}} \exp\left[\frac{eQ_d(z)}{aT_e} + \frac{e\varphi(z)}{T_e}\right], \quad (4)$$

$$I_{ste}(Q_d)=-\sqrt{8\pi} e a^2 n_{ste}(z) \sqrt{\frac{T_{ste}}{m_e}} \exp\left[\frac{eQ_d(z)}{aT_{ste}}\right]. \quad (5)$$

For the particle levitation in the sheath field, we take into account the sheath electrostatic force, the ion drag force, and gravity. Solution of the equation for the balance of forces together with the charging equation gives the dependence of the charge of the grain, levitating in the sheath electric field, as a function of its size, see rectangles in Fig. 2. Since the results were obtained for the parameters of the above experiment, we are able to compare them directly. We note a strong nonlinear dependence for the experimental and simulation curves, with the exponents to be sufficiently close (1.85 and 1.66 for the experiment, and 1.74 and 1.57 for the simulation). As an example of the contribution of STEs, triangles on Fig. 2(a) show the simulated charges of the levitating particles in the absence of hot electrons.

This effect demonstrates the nonlinear dependence of the levitating particles on the grain size when bigger and therefore heavier particles levitate deeper into the sheath (and closer to the electrode) where the fraction of energetic electrons is higher because of the secondary emission from the electrode. On the other hand, in the absence of STEs, the closer dust particle is to the electrode, the more pronounced is the deficit of thermal electrons because of the electrode's electric field. Indeed, by fitting the data without STEs, we see that the actual power index is 0.92, i.e., the slope of the dependence is decreasing. The analysis of these simulations demonstrates that out of various contributions (1) to dependence of  $Q_d$  on the particle's size we can single out the effect of  $f_T^\varphi$ . It is common to assume that the main electron temperature is not changing in the sheath region. Therefore the change of  $f_T^\varphi=f_{Te}^\varphi+f_{STE}^\varphi$  is due to the increased number of STEs closer to the electrode and the observed nonlinear dependencies are due to the different levitation heights of the particles with different sizes (and masses).

#### IV. DISCUSSION AND CONCLUSIONS

To elucidate the last statement, we experimented with particles made of different materials, i.e., particles with different densities. This allows us to have particles with similar sizes but different masses and therefore different levitation heights. Figure 3 shows the surface potential  $\varphi_s$  of various particles presented for the pressure  $P=8$  Pa and the input power  $W=64$  W. The surface potential for the particles made of the same material (melamine formaldehyde, circles in Fig. 3, see also fit solid line) is not constant with the varying size. Note that the values of the surface potentials of the particles made of corundum, carbon, and glass balloons in Fig. 3(a) are distinctively displaced with regard to values of the surface potential of the particles made of melamine formaldehyde. The surface potential of the more dense par-

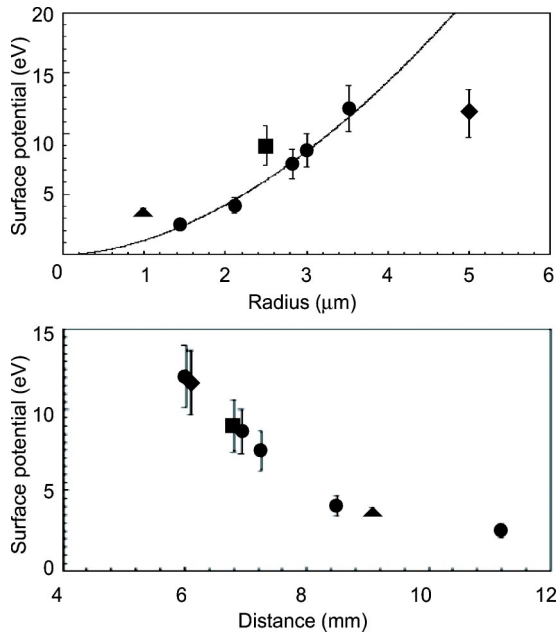


FIG. 3. Dependence of the surface potential on the particle radius (a) and on the levitation height (b). Circles stand for melamine formaldehyde, triangles for carbon, rectangles for corundum, and diamonds for glass balloons.

ticles is higher than that of a lighter particle of the same size and vice versa. This is in agreement with our earlier suggestion that the levitation height appears as the most important characteristic determining the size dependence of the charge. This becomes more clear if we consider the surface potential as the function of the levitation height, see Fig. 3(b). We can see that particles with different sizes levitating on the same height, for example, glass balloon with  $a=5 \mu\text{m}$  and melamine formaldehyde with  $a=3.5 \mu\text{m}$ , exhibit practically equal surface potentials. Figure 4 shows the calculated (on the basis of the model described above) dependencies for two distinctive cases of the surface potential of a levitating particle on its size. It is clearly seen that in the case of higher temperatures, the two-temperature character of the electron

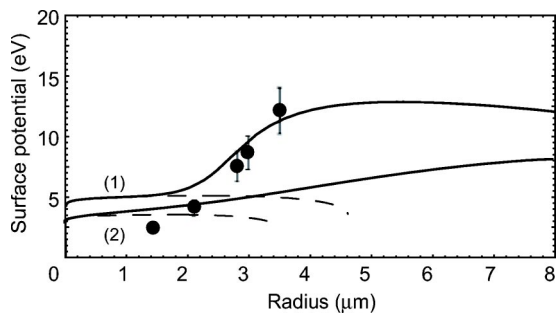


FIG. 4. Dependence of the surface potential of the levitating particle on its size for two different main electron temperatures: (1)  $T_e = 1.5 \text{ eV}$ ; (2)  $T_e = 1 \text{ eV}$ . The solid lines represent the dependence in the presence of STEs,  $T_{ste} = 8 \text{ eV}$ . The dashed lines are in the absence of STEs, they end at the maximum possible size for the particle levitation. The experimental dots are for melamine formaldehyde particles, see Fig. 3(a).

distribution reflects on the dependence of the surface potential. Indeed, the flat regions of almost constant potential correspond to the Boltzmann electron temperature (lower potential) and to the STE temperature (higher potential), respectively. For the second case, this character is smeared off by the weaker almost linear (within the range of sizes considered) dependence appearing as a spread out transition region between the two temperatures. We conclude that depending on the size range of particles and the plasma parameters, it is, in principle, possible to obtain different dependencies. In particular, for the results of Fig. 4, if the particle sizes in an experiment carried out under the first condition are less than  $2 \mu\text{m}$  or within the range  $4-8 \mu\text{m}$ , we obtain almost linear dependence of the particle charge on its size. On the other hand, for the lower temperature case, see curves (2) on Fig. 4, with  $T_e = 1 \text{ eV}$ , for all these ranges we have practically quadratic dependence of the particle charges on their sizes within the whole range up to  $8 \mu\text{m}$ .

For comparison, the experimentally obtained values of the surface potential for melamine formaldehyde particles are also plotted in Fig. 4. We see that a relatively good agreement is for particles larger than  $3 \mu\text{m}$ ; on the other hand, for smaller particles the experiment shows smaller values. We can attribute this discrepancy to the fact that the calculated character strongly depends on the model considered (in our particular case, the two-temperature Maxwell electron distribution function); for other types of the electron distribution, closer to those actually present in a particular experiment, other dependencies, closer to the experimental ones, can be obtained. It is important to stress, however, that the surface potential is not generally constant (and therefore the charge vs size dependence is not generally linear) even in the simplest case of the considered two-temperature Maxwellian distribution. We suggest that the constant surface potential appears most probably (if not only) for the one-temperature Maxwell distribution of the plasma electrons.

Recently, it was demonstrated [28] that even a small proportion of STEs is able to significantly influence the properties of the sheath. In the experiment [28], the presence of STEs was attributed to the features of the filament discharge. In the sheath of a rf-discharge plasma, despite vast number of experiments, possible presence of STE was not discussed yet. One of the reasons for that, according to our view, is that standard models [25,29] for rf discharge usually do not take into account the role of the secondary emission electrons, since most of the electron current through the sheath is capacitive displacement current. However, the ion-induced secondary electron emission from dc biased plasma electrodes is a well-known phenomenon which is required to sustain dc discharge [30]. In the case of rf discharge, due to strong ion flows to the negatively biased electrode, we should not expect secondary emission electrons to be absent. Of course, for normal rf biases ( $\sim 10-15 \text{ V}$ ), the yield coefficient is relatively small, less than 0.05 [23,24], but even in this case the influence of suprathermal electrons on the sheath properties and especially on the charging of macroscopic particles is profound. Indeed our simulations show that the sheath size and other characteristics such as plasma density distributions are strongly affected by STEs. This, together with the effect

of STEs on the particle charge, leads to the significant change of the levitation heights.

The strong dependence of the surface potential on the levitating particle's size reflects the dependence of the surface potential on the levitation distance from the electrode. This gives us an opportunity to employ dust particles as finite probes for determination of the electron distribution function; this goal, however, needs a more elaborated model for the sheath region. We stress here that the observed character of the charge (or the surface potential) vs size dependence can provide us information on the presence of energetic electrons in the sheath of rf discharge. Indeed, as we see from Fig. 4, in the absence of STEs, the surface potential demonstrates distinctively different behavior. Note also that the maximum possible levitation radius is decreased in the absence of STEs.

To conclude, we demonstrated that nonlinear dependence of the particle charge on its size observed in experiments can be explained by different plasma conditions in the sheath region where strong inhomogeneities of plasma parameters take place. Among the plasma parameters, the character of the electron distribution appears to be one of the most important for the particle charge. It is shown that the observed experimental data can be explained with good accuracy by the model dependencies based on the two-temperature electron distribution.

#### ACKNOWLEDGMENT

This work was supported by the Australian Research Council.

- 
- [1] H. Thomas, G.E. Morfill, V. Demmel, J. Goree, B. Feuerbacher, and D. Möhlmann, *Phys. Rev. Lett.* **73**, 652 (1994).
  - [2] J.H. Chu and I. Lin, *Phys. Rev. Lett.* **72**, 4009 (1994).
  - [3] V.A. Schweigert, I.V. Schweigert, A. Melzer, A. Homann, and A. Piel, *Phys. Rev. Lett.* **80**, 5345 (1998).
  - [4] A. Melzer, M. Klindworth, and A. Piel, *Phys. Rev. Lett.* **87**, 115002 (2001).
  - [5] H. Totsuji, T. Kishimoto, Ch. Totsuji, and K. Tsuruta, *Phys. Rev. Lett.* **88**, 125002 (2002).
  - [6] O.S. Vaulina, S.V. Vladimirov, O.F. Petrov, and V.E. Fortov, *Phys. Rev. Lett.* **88**, 245002 (2002).
  - [7] H.M. Thomas and G.E. Morfill, *Nature (London)* **379**, 806 (1996).
  - [8] E.C. Whipple, *Rep. Prog. Phys.* **44**, 1198 (1981).
  - [9] J. Goree, *Plasma Sources Sci. Technol.* **3**, 400 (1994).
  - [10] M.S. Barnes, J.H. Keller, J.C. Forster, J.A. O'Neill, and D.K. Coultas, *Phys. Rev. Lett.* **68**, 313 (1992).
  - [11] J.B. Pieper and J. Goree, *Phys. Rev. Lett.* **77**, 3137 (1996).
  - [12] A. Homann, A. Melzer, and A. Piel, *Phys. Rev. E* **59**, R3835 (1999).
  - [13] U. Konopka, L. Ratke, and H.M. Thomas, *Phys. Rev. Lett.* **79**, 1269 (1997).
  - [14] E.B. Tomme, D.A. Law, B.M. Annaratone, and J.E. Allen, *Phys. Rev. Lett.* **85**, 2518 (2000).
  - [15] V.E. Fortov, A.P. Nefedov, V.I. Molotkov, M.Y. Poustylnik, and V.M. Torchinsky, *Phys. Rev. Lett.* **87**, 205002 (2001).
  - [16] C. Zafiu, A. Melzer, and A. Piel, *Phys. Rev. E* **63**, 066403 (2001).
  - [17] A.A. Samarian, B.W. James, S.V. Vladimirov, and N.F. Cramer, *Phys. Rev. E* **64**, 025402(R) (2001).
  - [18] A.A. Samarian and B.W. James, *Phys. Lett. A* **287**, 125 (2001).
  - [19] E.B. Tomme, B.M. Annaratone, and J.E. Allen, *Plasma Sources Sci. Technol.* **9**, 87 (2000).
  - [20] A. Melzer, T. Trottenberg, and A. Piel, *Phys. Lett. A* **191**, 301 (1994).
  - [21] A. A. Samarian, S. V. Vladimirov, S. A. Maiorov, in *Dusty Plasmas in the New Millennium: Third International Conference on the Physics of Dusty Plasmas*, edited by R. Bharuthram *et al.* (AIP, Melville, NY, 2002), p. 410.
  - [22] S.V. Vladimirov, and N.F. Cramer, *Phys. Rev. E* **62**, 2754 (2000).
  - [23] A.V. Phelps and Z.L. Petrovic, *Plasma Sources Sci. Technol.* **8**, R21 (1999).
  - [24] D.M. Shaw, M. Watanabe, H. Uchiyama, and G.J. Collins, *Appl. Phys. Lett.* **75**, 34 (1999).
  - [25] M. A. Lieberman and A. J. Lichtenberg, *Principles of Plasma Discharges and Materials Processing* (Wiley, New York, 1994), pp. 454–460.
  - [26] C. Nairn, B.M. Annaratone, and J.E. Allen, *Plasma Sources Sci. Technol.* **7**, 478 (1998).
  - [27] V.N. Tsytovich, G.E. Morfill, and H. Thomas, *Plasma Phys. Rep.* **28**, 623 (2002).
  - [28] S. Takamura *et al.*, *Phys. Plasmas* **8**, 1886 (2001).
  - [29] Y. P. Raizer, *Gas Discharge Physics* (Springer, Berlin, 1991).
  - [30] J. Cobine, *Gaseous Conductors* (Dover, New York, 1958).